Metallophysics and Advanced Technologies
Металофіз. новітні технол.
Metallofiz. Noveishie Tekhnol.
2025, vol. 47, No. 1, pp. 83–102
https://doi.org/10.15407/mfint.47.01.0083
Reprints available directly from the publisher

PACS numbers: 46.35.+z, 61.72.Ff, 61.72.Mm, 62.20.fq, 81.20.Hy, 81.20.Wk, 83.50.Uv

Investigations on the Microstructure Evolution of Submicrocrystalline Metals Obtained by the Severe Plastic Deformation Method: A Review

B. S. Abdrasilov and B. B. Makhmutov

Karaganda Industrial University,
30 Republic Ave.,
KZ-101400 Temirtau, Republic of Kazakhstan

Currently, submicrocrystalline (SMC) metals and alloys obtained using severe plastic deformation (SPD) techniques are of increasing interest to researchers. In the present work, we focus on the study of materials with a disorientation spectrum dominated by large-angle grain boundaries, *i.e.*, not microfragmented, but nano- and micrograin materials—SMC materials in our terminology. The fundamental importance of the dominance of the high-angle grain boundaries (HAGBs) in the spectrum of grain-boundary disorientations is due to the exceptional role they play in the formation of the unique properties of SMC materials. As it will be shown in this paper, a special property of the HAGBs (in contrast to low-angle grain boundaries) is their ability to transition to a nonequilibrium state during SPD and to maintain this state for a certain time after deformation, which is the cause of many, if not all, special physical and mechanical properties of SMC materials.

Key words: severe plastic deformation, nanostructure, fragmentation, ultrafine-grained structure.

Нині субмікрокристалічні (СМК) метали та стопи, одержані з використанням методів інтенсивного пластичного деформування (ІПД), викликають підвищений інтерес у дослідників. У цій роботі ми зосередимося на

Corresponding author: Bolat Bizhanovych Makhmutov
E-mail: bb.makhmut@tttu.edu.kz

Citation: B. S. Abdrasilov and B. B. Makhmutov, Investigations on the Microstructure Evolution of Submicrocrystalline Metals Obtained by the Severe Plastic Deformation Method: A Review, *Metallofiz. Noveishie Tekhnol.*, **47**, No. 1: 83–102 (2025). DOI: 10.15407/mfint.47.01.0083

вивченні матеріялів зі спектром дезорієнтацій, у якому домінують великокутові межі зерен, тобто не мікрофраґментованих, а нано- і мікрозеренних матеріялів — СМК-матеріялів у нашій термінології. Принципове значення домінування висококутових меж (ВКМ) у спектрі дезорієнтацій меж зерен пов'язане з винятковою роллю, яку вони відіграють у формуванні унікальних властивостей СМК-матеріялів. Як буде показано в даній статті, особлива властивість ВКМ (на відміну від малокутових меж) — їх-ня здатність переходити в нерівноважний стан під час ІПД і зберігати цей стан упродовж певного часу після деформації, що є причиною багатьох, якщо не всіх, особливих фізико-механічних властивостей СМК-матеріялів.

Ключові слова: інтенсивна пластична деформація, наноструктура, фраґментація, ультрадрібнозерниста структура.

(Received 30 January, 2024; in final version, 8 July, 2024)

1. INTRODUCTION

When describing the structure of submicrocrystalline (SMC) materials, it is necessary to pay attention to the special state of other lattice defects—vacancies and dislocations. Although, in contrast to nonequilibrium grain boundaries, the role of these defects in the formation of properties is not determining, a number of peculiarities are observed in their behaviour.

If we start with point defects, first of all, we should note the exceptionally high concentration of nonequilibrium vacancies after SPD. Sometimes their concentration level reaches $C_v = 10^{-4}$ [1, 2]. It should be noted that these nonequilibrium vacancies are quickly annealed at long holding time or temperature increase and their contribution to the changes in the properties of SMC materials is usually insignificant.

Interesting features are also observed in the dislocation subsystem of SMC materials. First, it is a very high density of dislocations, the level of which is of $\sim 10^{15}$ m^2, which is two orders of magnitude higher than the usual one [3–7]. Secondly, due to the small grain size in SMC materials, there are difficulties in the operation of conventional intragrain sources of dislocations. The main mechanism of generation (nucleation) of dislocations in SMC materials is their generation from grain boundaries. This can lead to the emergence of special mesostructural regions—'regions of zero charge', the size of which exceeds the grain size (in contrast to conventional materials, where the region of zero charge, as a rule, is equal to the grain size).

Thirdly, despite the high density of dislocations, due to the small size of grains, very a few dislocations are contained in the grain body, and, during equal-channel angular pressing (ECAP), they do not form complex ensembles and clusters in the lattice and move through the

grains quite freely [8–12].

And, finally, the main thing: not only the generation of dislocations, but also the kinetics of dislocation motion in the grains and their 'disappearance' necessary to provide strain accommodation is determined by the interaction of dislocations with grain boundaries. This process is the key to understand the peculiarities of deformation behaviour of SMC materials.

In the case of SMC materials, all types of defects contribute to the deformation behaviour and structure evolution, but, in our opinion, nonequilibrium grain boundaries play a determining role. The description of the behaviour of nonequilibrium grain boundaries and their interaction with lattice dislocations is the key to understand the structure and properties of SMC materials.

Thus, the object of our study from the structural point of view are materials with a homogeneous submicrocrystalline structure with a spectrum of disorientations dominated by large angular grain boundaries, which (to ensure special physical and mechanical properties of the material) are in a nonequilibrium state.

2. PHYSICAL PROPERTIES OF SMC MATERIALS

Speaking about the physical properties of SMC materials, the most common are physical, electrical and thermal properties.

In Ref. [13, 14], a change—'shift'—of the Curie temperature by 36° (*i.e.*, approximately by $\cong 6\%$) and a 'shift' of the saturation magnetization value (by more than 30%) in the SMC nickel and iron were described. Except for the authors of the above-mentioned works, no one has ever recorded such 'shifts'. In our opinion, the 'effects' detected in [13, 14] are the result of insufficient care in setting up the experiments.

Note that the effect of a change in the Curie temperature was difficult to expect, since phase transitions of the second kind are associated with rearrangements in the electronic subsystem. Such rearrangements are very likely in dislocation nuclei and grain boundaries, but the fraction of the material in them in SMC structures is very small and cannot have a noticeable effect on the results of magnetic property measurements. Note also that, when heated to the Curie temperature (400°C for nickel, for example) due to the intense return of the defect structure, the density of dislocations 'returns' to the usual level, the grain size grows significantly and ceases to be submicron. Thus, any reasonable reason (under any bold assumptions about the role of defects) for the Curie temperature change disappears.

In a number of works [13, 15], another 'shift' has been recorded—a 2–4 times' increase of the coercivity after ECAP.

The 'shift' of the coercive force by several times compared to the undeformed state, as well as the intensive return of the coercive force

value during annealing, are quite typical for highly-deformed structures [16–21] and are not a specific effect related specifically to the ECA deformation and the creation of SMC structures.

It is known that the free path length of electrons in metallic materials, as a rule, does not exceed several nanometres. This value is significantly smaller than the characteristic size of the structural elements of SMC materials ($\cong 100$ nm). This means that the fundamental electrical properties of materials cannot change after ECAP.

In experiments, a noticeable increase ('shift') of electrical resistivity, which sometimes reaches ten percent at room temperature, is often observed. This is because the large density of lattice defects in SMC materials affects the electrical conductivity. The magnitude of the conductivity changes associated with lattice defects can be easily estimated using tabulated values of the resistivity of lattice defects. For copper, for example, the resistivity of defects is equal to the following, respectively: for vacancies, $D_r = 2{\cdot}10^{-8}$ Ohm·m per 1% of vacancies, for, dislocations $D_r = 2.8{\cdot}10^{-19}$ Ohm·cm^3, and for grain boundaries, $D_r \cong 4{\cdot}10^{-12}$ Ohm·cm^2.

At the limiting values of defect concentration in SMC copper, grain size $d \cong 200$ nm, dislocation density $r_v \cong 10^{11}$ cm^2 and vacancy concentration $C_v = 10^{-4}$, the defect-related increase in electrical resistivity at room temperature reaches $\cong 2.5{\cdot}10^{-9}$ Ohm·cm, which is of about 10% of the standard value. The relative contributions of various lattice defects to this change are as follow: the contribution of grain boundaries is of $\cong 2{\cdot}10^{-9}$ Ohm·cm, the contribution of dislocations is of $2.3{\cdot}10^{-10}$ Ohm·cm, and the contribution of vacancies is of about $2{\cdot}10^{-10}$ Ohm·cm.

It follows from the estimates that the main role in the experimentally measured 'shift' of electrical resistivity in SMC materials is played by grain boundaries [22–25].

It also follows from the estimates that the effect of the 'shift' of the electrical resistance level after ECA deformation observed in the experiments is trivially described within the framework of traditional ideas about the influence of defects on the electrical conductivity of metal and is not a specific property of SMC materials.

The thermal properties of SMC materials are usually studied by differential scanning calorimetry (DSC) [1, 2, 26]. The magnitude of heat release during heating of SMC materials with an initial grain size of $\cong 0.1 \times 0.2$ μm^2 is at the level of $\cong 1$ J/g [27]. This is a rather high value and one can speak about some 'shift'. In accordance with classical ideas [42], heat generation during heating is related to the return of defect structure. The contributions of various types of defects to heat release are calculated based on standard estimates of the energy of individual defects. It is known that the energy per unit length of a lattice dislocation is $\approx CA^2/4\pi(1-\nu)\ln(R/r_0)$, and the energy per unit area of a grain boundary is $\gamma_b \approx G_b/24$ [28]. Using these values and determining exper-

imentally the values of structural parameters (grain size and dislocation density), it is not difficult to determine the contributions to heat release associated with each type of defect. The difference between the calculated value and the experimentally measured value is usually associated with the contribution of vacancies. Taking the energy of vacancy formation equal to $\cong 10kT_m$ [45], the corresponding vacancy concentration is determined. In SMC materials, it turns out to be at a high level, but in general, reasonable for highly deformed structures: $C_v \sim 10^{-4}$ [1, 2]. Estimates show that the observed 'shift' in heat release is a trivial effect associated with the increased defectiveness of NMC materials. This is also evidenced by the fact that the shape of the DSC heat release curves (and the scale of the effect) is similar to the DSC curves obtained for conventional highly deformed structures [15].

So, in materials subjected to ECAP, some 'shifts' in the parameters characterizing physical properties are indeed observed, compared to undeformed materials. However, and this is important to emphasize, these changes are quite trivial. They fully correspond to the expected and easily calculated within the framework of classical concepts—changes in structure-sensitive parameters, when defects are introduced into the material. As a rule, the scale of these changes corresponds to the scale of changes in the specified parameters in materials subjected to deformation by other methods. As a rule, the observed 'shifts' are associated not only with the small grain size of SMC materials, but also with an increased density of lattice dislocations and a high concentration of vacancies [29–33].

Thus, the mentioned 'shift effects' of physical properties in SMC materials occur, but are trivial. Note that their study can help in solving problems of estimating the density of individual types of defects, especially, in the case of complex use of different methods.

At the same time, it should be noted that, in SMC materials, a number of effects are observed that are characteristic only of this group of materials. Such effects are observed in SMC materials in the case, when the process under study depends on several parameters, which, in turn, depend differently on the grain size d. In the case, where a change in d leads to multidirectional changes in parameters, a situation is possible, when, at a certain d^*, a maximum or minimum appears in the dependence of process parameters on grain size. An example of such an effect is the behaviour of SMC materials during deformation in the superplasticity regime. This effect is manifested in the fact that maximum plasticity is observed not in metals with smaller grain sizes—as follows from traditional ideas about the mechanisms of superplasticity [34, 35], but in materials with an 'intermediate' grain size d, lying close to $\cong 1$ μm [36–39]. This result is inexplicable within the framework of the classical theory of superplasticity [34, 35].

Another example of a similar effect is the amazing property of some

SMC materials, under tensile conditions at room temperatures, to simultaneously show a significant increase in strength and increase in ductility [3, 40, 41–43]. In conventional materials, an increase in strength, as a rule, leads to a decrease in ductility, and in some SMC materials, and specifically in the grain size range of 0.5–1 μm, a simultaneous increase in strength and ductility at room temperature is observed.

The third example very widely discussed in the literature [44–46] is associated with the behaviour of the yield stress of SMC materials. In accordance with the generally accepted model, the yield strength is related to the grain size by the Hall–Petch relation $\sigma_T = \sigma_0 + K/d^{-1/2}$, and, therefore, a decrease in grain size d should lead to an increase in the yield strength σ_T [44]. However, in the field of SMC materials, this law ceases to be observed. In some cases, a weak dependence of σ_T on d is observed [45, 46], and, in other cases, an inverse relationship is observed: the smaller d, the smaller σ_T [46, 47].

Thus, as can be seen from the brief analysis, SMC materials have special properties and a whole range of specific effects are observed in them, which makes it possible to distinguish these materials into a separate class of structural materials.

Separately, we should touch upon the problem of the formation and thermal stability of the structure of SMC materials during SPD and subsequent annealing. It should be noted that most of the experimental results obtained related to the study of diffusion-controlled processes in SMC materials are incomplete and contradictory. Often, for the same metal obtained by the same SPD method under the same conditions, conflicting data are provided on the influence of grain size and the state of grain boundaries on the nature and kinetics of diffusion-controlled processes, the influence of the structure of grain boundaries on mechanical, diffusion, magnetic, electrical, and other properties. This does not allow us to systematize the results and build correct theoretical models that describe the patterns observed in experiments and provide a satisfactory comparison.

A particularly difficult situation arises in the issue of describing diffusion-controlled processes of grain dispersion, recrystallization and decomposition of the solid solution in SMC materials.

Currently, there is a fairly large number of works in the literature devoted to the study of the laws of the process of dispersion of the structure of metals during SPD [3, 13, 46]. As known, developed plastic deformation is accompanied by intense fragmentation—the formation of misoriented microrange-fragments in the material [48]. As deformation occurs, the misorientation of fragments increases, and their sizes gradually decrease, reaching a certain minimum value d^*, which is usually called the limit of deformation refinement or the limit of grain dispersion [48].

Analysis of literature data [3, 48, 49] shows that the value of the

dispersion limit d^* depends on the structure and properties of the material, as well as on the selected SPD mode: the deformation pattern, its rate and temperature.

One of the most important factors is the deformation temperature. Its influence on the dispersion limit has been studied in detail for the aluminium and magnesium alloys [50, 51]; isolated studies have been carried out for copper [52], iron [53], nickel [54], titanium [55], *etc*. Generalization of these data allows us to conclude that the value of the dispersion limit d^* monotonically increases with increasing deformation temperature.

Studies by a number of authors [3, 51, 52] show that the dependence $d^*(T)$ in some cases has a two-stage character. In the temperature range above temperature T_1, which can conventionally be called the recrystallization temperature during ECAP, d^* increases with increasing temperature very intensively. In a number of works, the authors note a more complex nature of the dependence of d^* on the SPD temperature, which, according to the authors of Ref. [56], is caused by a change in the mechanisms of grain refinement with increasing temperature.

To describe the features of structure formation in metals and alloys during SPD, noteworthy works are those that consider the fragmentation process from the point of view of the concept of dynamic recrystallization during SPD [54], works that describe the process of grain structure refinement and the formation of high-angle grain boundaries using methods for numerical modelling of the nucleation and further development of low-angle subboundaries [57], ideas about the peculiarities of fragmentation processes at the mesolevel, the possibility of calculating the value of the limit of grain dispersion based on ideas about the accommodative nature of the SPD process. They deserve special attention and theoretical works based on the traditional language of the theory of disclinations in solids [58].

Thus, despite a large number of experimental works devoted to studying the process of formation of SMC structures using SPD methods, the question of the mechanisms of fragmentation of the grain structure of metals and alloys, as well as the question of the reasons for the existence of the grinding limit and the theoretical calculation of its value have not yet been resolved. In our opinion, among the key theoretical questions, which should be clarified in this discussion, is the question of the mechanism of formation of large grain boundaries during SPD, without an answer to which, further discussion about the mechanisms of fragmentation during SPD is very difficult [59–63].

3. CONTINUOUS DYNAMIC RECRYSTALLIZATION

In recent years, a large amount of experimental evidence has appeared for the formation of *BAB* during deformation through the rotation of

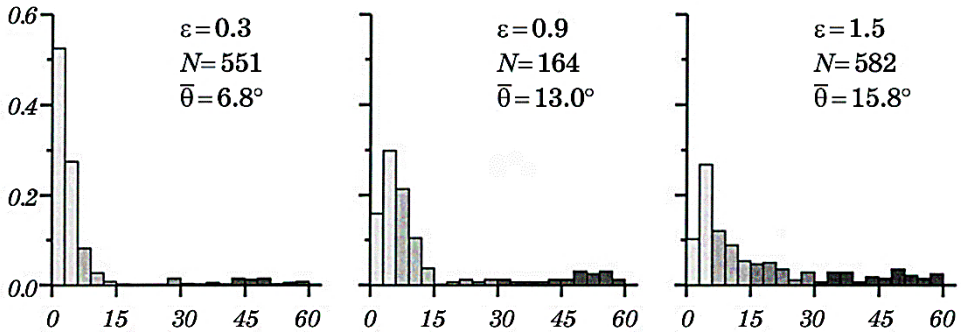

Fig. 1. Increase in the misorientation angle of grains with increasing degree of hot deformation in the aluminium–copper alloy (ε is the degree of deformation, N is the number of measurements, $\bar{\theta}$ is the average misorientation angle) [65].

subgrains (Fig. 1). In this case, the microstructure is formed quite homogeneous throughout the entire volume of the material, and it is difficult to identify specific places of nucleation and growth of nuclei. This phenomenon is classified as continuous dynamic recrystallization (CDR) [64]. The phenomenon of CDR has been much less studied compared to DDR; this is due both to the difficulties of identifying the onset of recrystallization (the study became possible only with the development of EBSD technology) and to the need to create a high level of deformation in the material, which is not realized in simple tensile or compression experiments. Most often, an SPD is required to begin the CDR process. To date, the overwhelming number of works devoted to the study of CDR processes is related to SPD processes.

Basic experimental facts about CDR (Fig. 2) [66] are as follow.

1) LPC has the form of a curve with saturation (Fig. 2, *a*), in some materials the appearance of one peak is observed, but more often there is no peak. The total strain accumulated over several cycles is most often plotted along the strain axis. The flow stress at the steady stage decreases with increasing temperature [66] increases with increasing strain rate [67] and does not depend on the initial grain size [68].

2) The average value of grain misorientation increases with increasing degree of deformation; low deformation rates accelerate this process [69]. However, there are stable misorientations that do not transform into HAGBs [66] (Fig. 2, *b*).

3) The transformation of LAB into HAGBs occurs as a result of a gradual increase in misorientations (HIM), rotation of the lattice near the grain boundary (LRCA) or the formation of microbend bands (MSBs), as shown schematically in Fig. 2, *c* [70].

4) The average grain size decreases with increasing deformation and reaches a saturation value at high degrees of deformation (Fig. 2, *d*). In

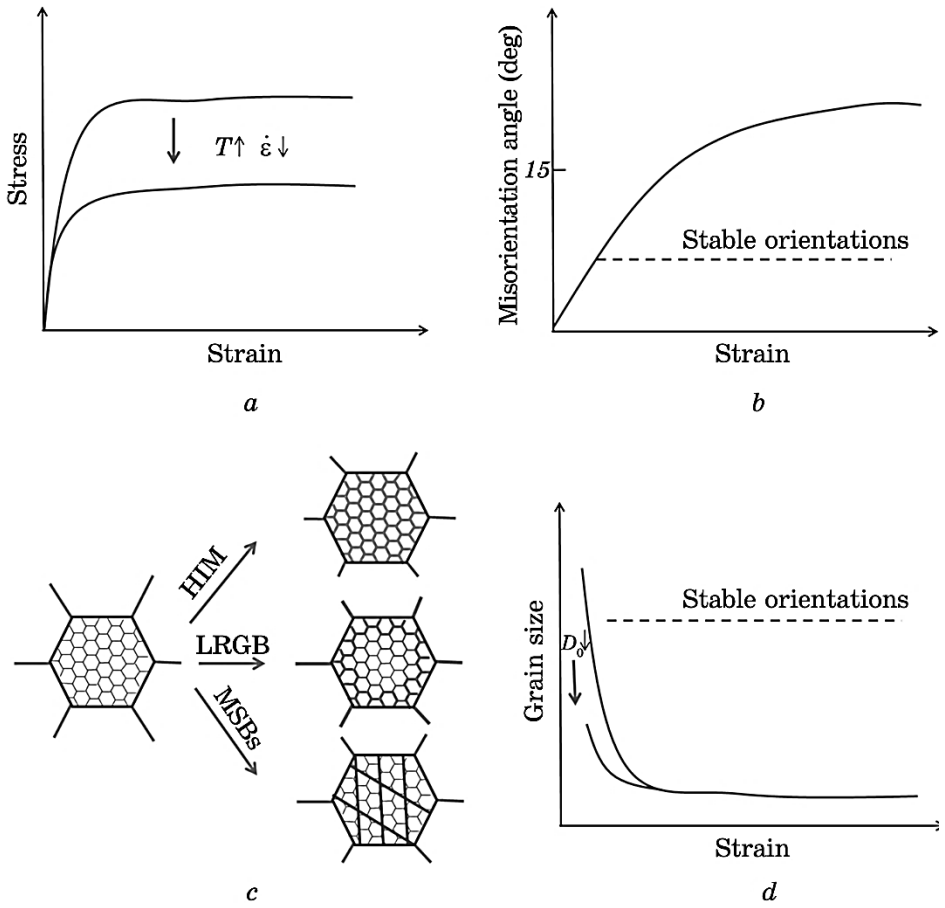

Fig. 2. Schematic representation of typical experimentally observed phenomena during CDR: DDR (*a*); change in the average value of CA rotation at elevated ($> 0.5T_m$) temperatures (*b*); transformation of LAGBs into HAGBs with a homogeneous increase in the misorientation angle, rotation of the lattice in the boundary region, or formation of ROP (thin lines indicate LAGBs, thick lines indicate HAGBs) (*c*); evolution of the average grain size with increasing degree of deformation (*d*) [71].

this case, the preservation of individual initial grains, favourably oriented to stress, is observed, even at high degrees of deformation. Reducing the initial grain size can lead to acceleration of the kinetics of grain refinement at high degrees of deformation. In this case, the method of strain accumulation has a very weak effect on the kinetics of the CDR process [65].

5) At high degrees of deformation during CDR, a strong crystallographic texture is formed in the material [65, 72].

CDR with a Gradual Increase in Grain Misorientation. At relatively high deformation temperatures ($> 0.5T_m$), as a rule, a homogeneous microstructure is formed; deformed grains or shear bands are formed less frequently than during cold deformation. Under these conditions, the CDR process begins due to the accumulation of dislocations in the MG, because of which their misorientation increases until a critical angle is reached ($\cong 15°$). Since it is difficult to track changes in the misorientation of an individual boundary, as a rule, they talk about the average value for the ensemble. A similar mechanism is observed experimentally both during deformation of a polycrystalline material and in the case of single crystals.

This type of dynamic recrystallization (DR) is observed during SPD with degrees of deformation of 2 and higher. The mechanism of occurrence is the formation of dislocation cells, which are transformed with increasing degree of deformation into subgrains and finally into grains (Fig. 3). Figure 3 shows the experimental dependences of grain size, average grain misorientation angle, and dislocation density at subboundaries during hot all-round forging of pure copper [72].

CDR during Progressive Lattice Rotation near Grain Boundaries. There is evidence that CDR can occur through progressive rotation of subgrains adjacent to pre-existing grain boundaries. This process is similar to the so-called rotational recrystallization described for many

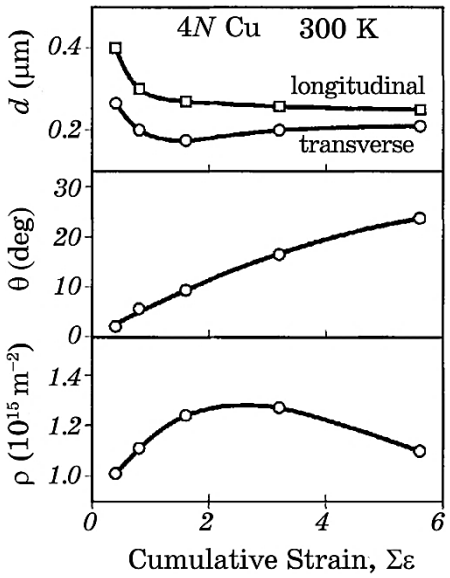

Fig. 3. Dependences of grain size, average grain misorientation angle and dislocation density in subboundaries during hot all-round forging of pure 4*N* copper [72].

crystalline materials [73].

Today, a simple mechanism has been proposed to explain the formation of new grains during hot deformation of h.c.p. metals (Fig. 4) [74]. Deformation in h.c.p. materials is inhomogeneous due to the absence of independent slip systems; therefore, local shear often begins near the grain boundary (Fig. 4, *a*). As the local shear develops, the CA rotates. In this case, the flowing DW (Fig. 4, *b*) promotes the formation of new small subgrains near the original CA (Fig. 4, *c*). As a result, the accumulation of a large number of subgrains leads to their merging and the formation of new grains surrounded by HAGBs. Figure 5 shows photographs of the microstructure formed according to the above mechanism [69, 74].

In Ref. [75], models of CDR micromechanisms were developed that predict the grain size distribution, the evolution of the misorientation angle, the crystallographic texture, and the strain hardening of the material during hot intense deformation. The main assumption of these models is that the lattice inside the individual grain is not homogeneous during severe deformation. Near the grain boundary, local lattice distortions arise due to the accumulation in the grain bounda-

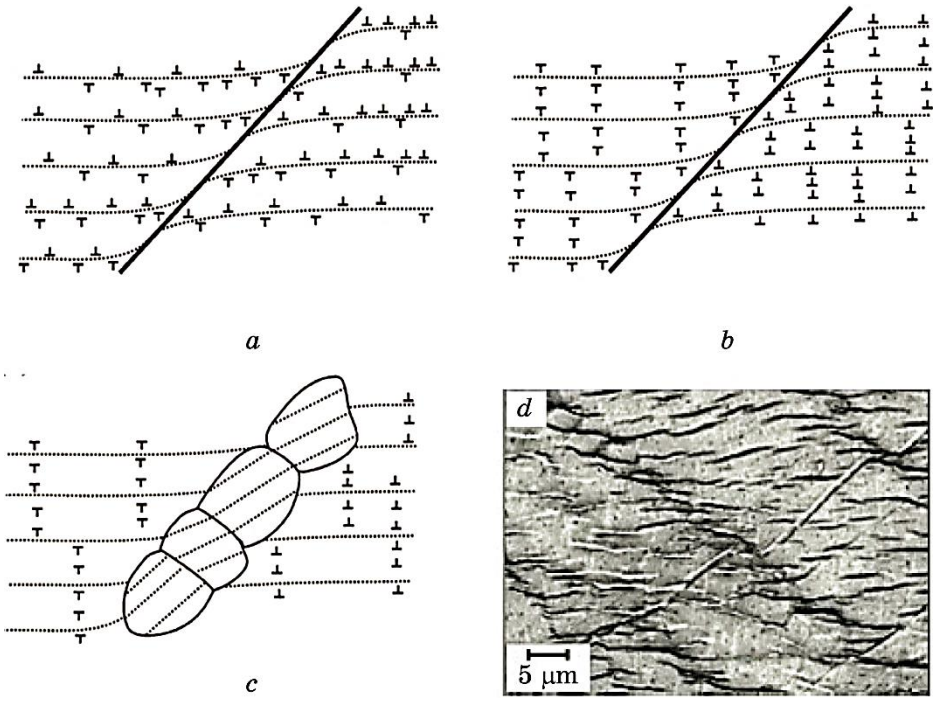

Fig. 4. Schematic representation of the formation of a chain of small grains along the CA in magnesium [74].

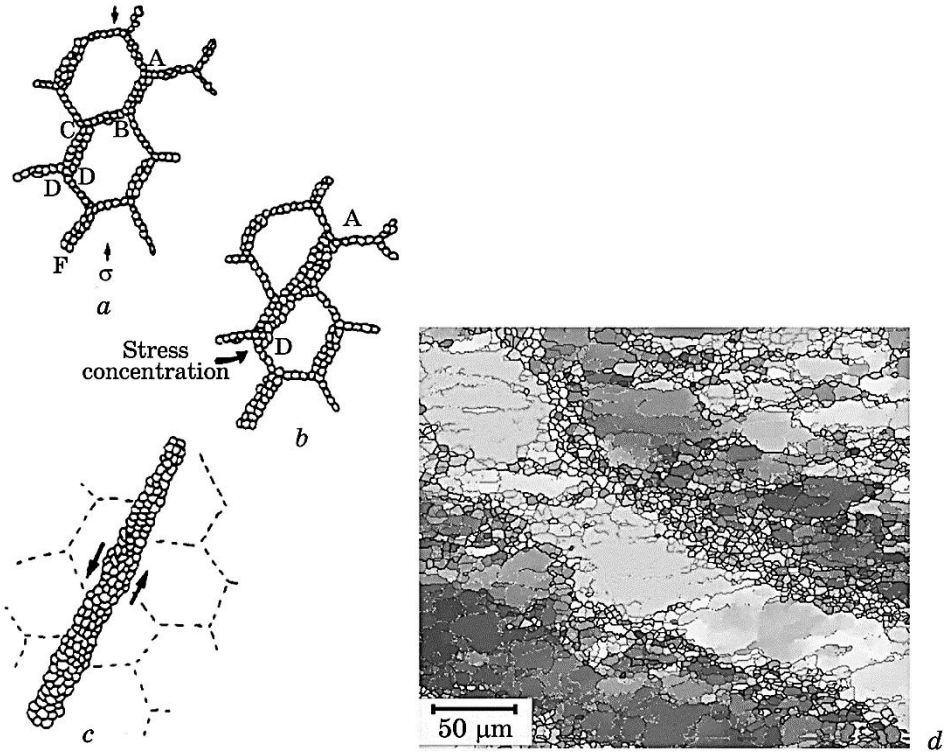

Fig. 5. Formation of a strip of small grains along the boundaries according to the mechanism shown in Fig. 4 [74] (*a*–*c*); EBSD maps of the grain structure of a magnesium alloy [69] (*d*).

ries of products of delocalization of defects that enter the boundary during the deformation process. These distortions increase as the degree of deformation increases (Fig. 6). When a certain critical degree of bending is reached, because of rotation of the central part, the centre and periphery are separated by a boundary. The constructed model well describes the flow of CDR in aluminium alloys. Figure 7 shows a TEM image of the crystal structure of the material, showing lattice distortion near the CA [76]. It is shown that the real deviation of the plane from the straight line can reach 5°.

CDR occurring in the presence of microshear bands (MSBs). The formation of MSBs during hot deformation is observed in images obtained using optical, scanning and transmission microscopy, as well as EBSD [64, 74, 77].

Numerous MSBs, forming in the grain body, lead to the appearance of a MSB network, creating misoriented fragments with their intersections (Figs. 8, 9) [77]. Further deformation leads to an intensive increase in the number of MSBs and the formation of LAGBs and HAGBs

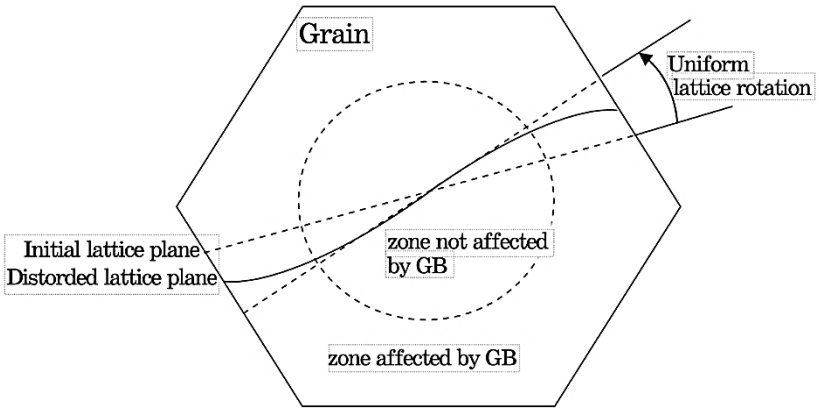

Fig. 6. Scheme of curvature of the crystallographic plane during grain rotation [75].

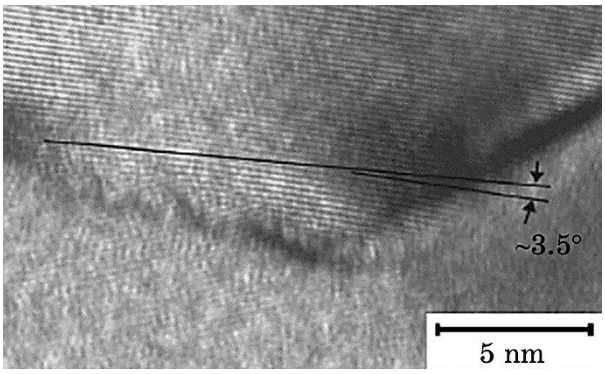

Fig. 7. Experimental confirmation of the basic assumption of the Tyth model [76].

between the fragments. Thus, the proportion of equiaxed grains of small size increases, gradually filling the entire volume.

It has been shown that a similar mechanism for the nucleation of small grains is observed, when the direction of deformation changes. ECAP can be considered the most striking example in this case.

4. GEOMETRIC DYNAMIC RECRYSTALLIZATION

The geometric dynamic recrystallization (GDR) process has been described in a wide range of metallic materials, including pure metals, solid-solution strengthened alloys, and particle-strengthening materials [78–81]. Moreover, although a number of authors combine GDR

with CDR, there are differences between these processes [71, 82].

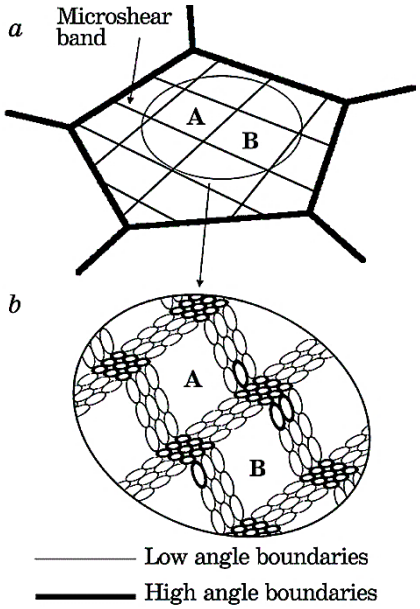

Fig. 8. Scheme of the formation of a fine-grained structure, when crossing the MSB [69].

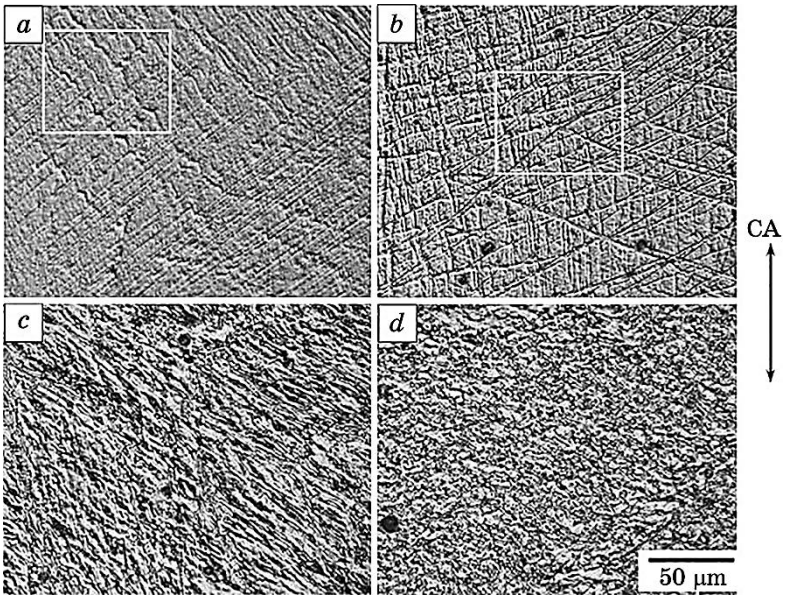

Fig. 9. Experimental observation of the formation of new small grains at the intersection of MSB [69].

Below, there are the main experimental characteristics of the GDR.

1. GDR is most often observed for materials with medium and high SFE, deformed at elevated temperatures with a low deformation rate. At low temperatures, the DB dominates, since the steps on the CA limit their mobility. At very high temperatures, grain boundaries are so mobile that hardening does not have time to generate new grains. Thus, to implement GDR, a certain temperature optimum is required [78].

2. Subgrains are formed after reaching a critical level of deformation and remain constant in size throughout the entire deformation process. The size of subgrains at the saturation stage decreases with increasing parameter 3-X [83].

3. The amount of misorientation of part of the subgrains at the saturation stage during GDR differs significantly from that observed in the case of CDR and remains constant at a level of about 2°. In the case of GDR, a bimodal distribution of grain misorientations is always observed [84].

4. During the GDR process, the original texture remains virtually unchanged. In some experiments, a slight softening of the texture is observed, which leads to a smoothing of the LPC peak [78].

GDR is described as the process of formation of equiaxed grains during hot deformation under the following conditions:

1. presence of a selected direction of deformation;
2. CA can migrate to form steps;
3. during the deformation process, grain thinning is observed in one or two directions;
4. bends on the *BAB* can interact, when the grain width reaches 2–3 subgrain sizes.

The above-mentioned GDR mechanism is based only on the idea of microstructure evolution depending on the initial grain size and the selected direction of stress application. In reality, there are also some other aspects that need to be taken into account.

Firstly, during deformation, bends should form on the grain boundaries, which cannot be taken into account, when modelling grains as spheres or cubes. Let us consider the process of bending formation. During hot deformation, subgrain boundaries first appear near the initial boundaries. Steps appear on both sides of the boundary in the process of local migrations of grain boundaries at the junctions with subgrain boundaries formed during DV. Since the grain thickness is not constant along the long axis, GDR does not occur simultaneously upon reaching a critical level of deformation. Some parts of the grain reach critical stress earlier and, in them, GDR begins first. Secondly, a high degree of deformation in the selected direction is required [84].

Although the mechanisms of GDR are mostly understood and have been experimentally discovered in many metals and alloys, attempts to

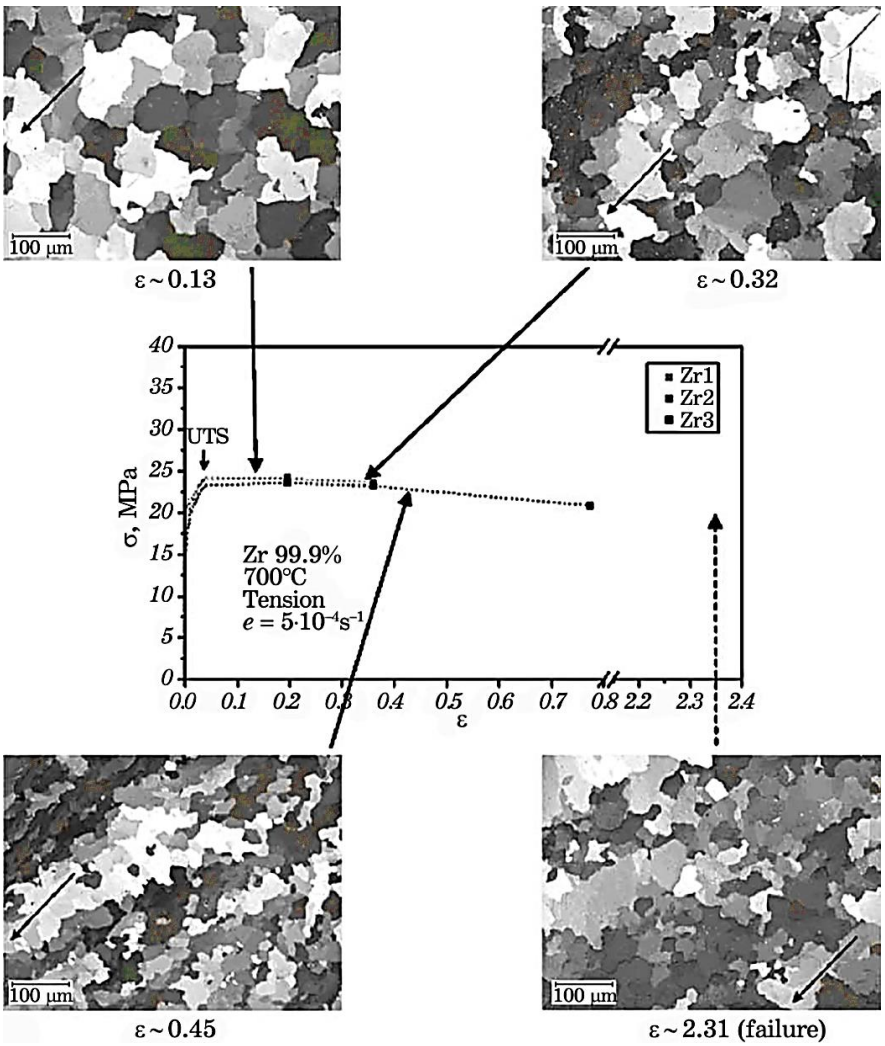

Fig. 10. Evolution of the α-Zr microstructure during rolling at 700°C [86].

construct a model of this process are based not on physical, but on geometric principles [82]. In general, these models predict microstructure evolution well.

Figure 10 shows snapshots of the microstructure evolving during the GDR process [86].

5. CONCLUSION

The results of studies of the influence of the structural state of grain

boundaries of SMC metals on the peculiarities of the return and recrystallization processes during annealing can be used to determine the optimal modes of equal-channel angular pressing and heat treatment of SMC metals. Optimal modes of production and processing of metals and alloys allow to ensure the formation of SMC structure with high thermal stability (high temperature of the beginning of recrystallization), low tendency to abnormal grain growth leading to the formation of inhomogeneous (heterogeneous) structure, high strength characteristics, *etc*.

REFERENCES

1. D. Setman, E. Schafler, E. Korznikova, and M. J. Zehetbauer, *Mater. Sci. Eng. A*, **493**: 116 (2008).
2. W. Q. Cao, C. F. Gu, E. V. Pereloma, and C. H. J. Davies, *Mater. Sci. Eng. A*, **492**: 74 (2008).
3. A. Volokitin, A. Naizabekov, I. Volokitina, and A. Kolesnikov, *J. Chem. Technol. Metall.*, **57**, Iss. 4: 809 (2022).
4. I. E. Volokitina, *Met. Sci. Heat Treat.*, **63**, Nos. 3–4: 163 (2021).
5. A. B. Naizabekov, S. N. Lezhnev, and I. E. Volokitina, *Met. Sci. Heat Treat.*, **57**, Nos. 5–6: 254 (2015).
6. A. Naizabekov, A. Arbuz, S. Lezhnev, E. Panin, and I. Volokitina, *Phys. Scr.*, **94**, No. 10: 105702 (2019).
7. I. E. Volokitina and A. V. Volokitin, *Metallurgist*, **67**: 232 (2023).
8. I. Volokitina, A. Bychkov, A. Volokitin, and A. Kolesnikov, *Metallogr., Microstruct., Anal.*, **12**: 564 (2023).
9. S. Lezhnev, I. Volokitina, and T. Koinov, *J. Chem. Technol. Metall.*, **49**, Iss. 6: 621 (2014).
10. I. Volokitina, *J. Chem. Technol. Metall.*, **55**, Iss. 2: 479 (2020).
11. A. Naizabekov, S. Lezhnev, E. Panin, A. Arbuz, T. Koinov, and I. Mazur, *J. Mater. Eng. Perform.*, **28**: 200 (2019).
12. B. Sapargaliyeva, A. Agabekova, G. Ulyeva, A. Yerzhanov, and P. Kozlov, *Case Studies in Construction Materials*, **18**: e02162 (2023).
13. R. Z. Valiev and I. V. Alexandrov, *Nanostrukturirovannyye Materialy, Polucheennyye Metodom Intensivnoy Plasticheskoy Deformatsii* [Nanostructured Materials Obtained by Severe Plastic Deformation] (Moskva: Logos: 2000) (in Russian).
14. R. Z. Valiev, A. V. Korznikov, and R. R. Mulyukov, *Fiz. Met. Metalloved.*, **76**, No. 4: 70 (1992) (in Russian).
15. K. Y. Mulyokov, G. F. Korznikova, R. Z. Abdulov, and R. Z. Valiev, *J. Magn. Magn. Mater.*, **89**: 207 (1990).
16. M. Latypova, V. Chigirinsky, and A. Kolesnikov, *Prog. Phys. Met.*, **24**, No. 1: 132 (2023).
17. N. Vasilyeva, R. Fediuk, and A. Kolesnikov, *Materials*, **15**: 3975 (2022).
18. I. E. Volokitina, *Met. Sci. Heat Treat.*, **62**: 253 (2020).
19. I. E. Volokitina, A. V. Volokitin, and E. A. Panin, *Prog. Phys. Met.*, **23**, No. 4: 684 (2022).
20. A. Naizabekov, A. Volokitin, and E. Panin, *J. Mater. Eng. Perform.*, **28**: 1762

(2019).
21. I. Volokitina, A. Volokitin, A. Denissova, Y. Kuatbay, and Y. Liseitsev, *Case Studies in Construction Materials*, **19**: e02346 (2023).
22. V. V. Chigirinsky and Y. S. Kresanov, *Metallofiz. Noveishie Tekhnol.*, **45**, No. 4: 467 (2023).
23. E. Panin, Z. Gelmanova, and Y. Liseitsev, *Case Studies in Construction Materials*, **19**: e02609 (2023).
24. N. Zhangabay, I. Baidilla, A. Tagybayev, Y. Anarbayev, and P. Kozlov, *Case Studies in Construction Materials*, **18**: e02161 (2023).
25. A. Nayzabekov and I. Volokitina, *Phys. Met. Metallogr.*, **120**: 177 (2019).
26. N. M. Amirkhanov, R. K. Islamgaliev, and R. Z. Valiev, *Phys. Met. Metallogr.*, **86**: 296 (1998).
27. M. Goto, S. Z. Han, T. Yakushiji, S. S. Kim, and C. Y. Lim, *Int. J. Fatigue*, **30**: 1333 (2008).
28. M. F. Ashby, C. Gandli, and D. M. R. Taplin, *Acta Metall.*, **27**: 699 (1979).
29. I.E. Volokitina, *Prog. Phys. Met.*, **24**, No. 3: 593 (2023).
30. I. Volokitina, A. Volokitin, and D. Kuis, *J. Chem. Technol. Metall.*, **56**: 643 (2021).
31. I. E. Volokitina and G. G. Kurapov, *Met. Sci. Heat Treat.*, **59**, Nos. 11–12: 786 (2018).
32. S. Lezhnev, E. Panin, and I. Volokitina, *Adv. Mat. Res.*, **814**: 68 (2013).
33. S. Lezhnev, A. Naizabekov, E. Panin, and I. Volokitina, *Procedia Eng.*, **81**: 1499 (2014).
34. T. G. Nieh, D. Wadsworth, and O. D. Sherby, *Superplasticity in Metals and Ceramics* (Cambridge: Cambridge Univ. Press: 1997).
35. V. N. Perevezentsev, V. V. Rybin, and V. N. Chuvil'deev, *Acta Metall. Mater.*, **40**: 887 (1992).
36. R. K. Islamgaliev, N. F. Yunusova, R. Z. Valiev, N. K. Tsenev, V. N. Perevezentsev, and T. G. Langdon, *Scr. Mater.*, **49**, Iss. 5: 467 (2003).
37. R. K. Islamgaliev, N. F. Yunusova, and R. Z. Valiev, *Nanostructures Materials by High-Pressure Revere Plastic Deformation* (Springer: 2006), p. 299–304.
38. S. H. Kang, Y. S. Lee, and J. H. Lee, *J. Mater. Process. Technol.*, **201**: 436 (2008).
39. A. V. Sergueeva, N. A. Mara, R. Z. Valiev, and A. K. Mukherjee, *Mater. Sci. Eng. A*, **410–411**: 413 (2005).
40. R. Z. Valiev and I. V. Aleksandrov, *Doklady Physics*, **46**: 633 (2001).
41. A. Yamashita, Z. Horita, and T. G. Langdon, *Mater. Sci. Eng. A*, **300**: 142 (2001).
42. H. K. Kim and W. J. Kim, *Mater. Sci. Eng. A*, **385**: 300 (2004).
43. Y. Wang, M. Chen, F. Zhou, and E. Ma, *Nature*, **419**: 912 (2002).
44. A. P. Zhilyaev, A. A. Gimazov, E. P. Soshnikova, A. Rezesz, and T. G. Langdon, *Mater. Sci. Eng. A*, **489**: 207 (2008).
45. E. Shafler and R. Pippan, *Mater. Sci. Eng. A*, **387–389**: 799 (2004).
46. H. Conrad and K. Jung, *Scr. Mater.*, **53**: 581 (2005).
47. M. A. Meyers, A. Mishra, and D. J. Benson, *Prog. Mater. Sci.*, **51**: 427 (2006).
48. V. M. Segal, *Mater. Sci. Eng. A*, **197**: 157 (1995).
49. V. Y. Gertsman, R. Birringer, R. Z. Valiev, and H. Gleiter, *Scr. Met. Mat.*, **30**: 229 (1994).
50. A. Goloborodko, O. Sitdikov, R. Kaibyshev, H. Miura, and T. Sakai, *Mater. Sci.*

Eng. A, **381**: 121 (2004).
51. Y. C. Chen, Y. Y. Huang, C. P. Chang, and P. W. Kao, *Acta Mater.*, **51**: 2005 (2003).
52. W. H. Huang, C. Y. Yu, P. W. Kao, and C. P. Chang, *Mater. Sci. Eng. A*, **356**: 321 (2004).
53. D. H. Shin, J. J. Pak, Y. K. Kim, K. T. Park, and Y. S. Kim, *Mater. Sci. Eng. A*, **325**: 31 (2002).
54. S. Lezhnev and A. Naizabekov, *J. Chem. Technol. Metall.*, **52**, No. 4: 626 (2017).
55. G. I. Raab, E. P. Soshnikova, and R. Z. Valiev, *Mater. Sci. Eng. A*, **387–389**: 674 (2004).
56. V. M. Segal, I. J. Beyerlein, C. N. Tome, V. N. Chuvil'deev, and V. I. Kopylov, *Fundamentals and Engineering of Severe Plastic Deformation* (New York: Nova Science Publishers: 2010).
57. V. N. Perevezentsev and G. F. Sarafanov, *Rev. Adv. Mater. Sci.*, **30**: 73 (2012).
58. S. V. Bobylev, M. Yu. Gutkin, and I. A. Ovid'ko, *Acta Mater.*, **52**: 3793 (2004).
59. A. Volokitin, I. Volokitina, and E. Panin, *Metallogr., Microstruct., Anal.*, **11**, No. 4: 673 (2022).
60. S. Lezhnev, A. Naizabekov, I. Volokitina, and A. Volokitin, *Procedia Eng.*, **81**: 1505 (2014).
61. I. E. Volokitina, *Met. Sci. Heat Treat.*, **61**: 234 (2019).
62. S. N. Lezhnev, I. E. Volokitina, and A. V. Volokitin, *Phys. Met. Metallogr.*, **118**, No. 11: 1167 (2017).
63. I. Volokitina, *J. Chem. Technol. Metall.*, **57**: 631 (2022).
64. T. Sakai, A. Belyakov, R. Kaibyshev, H. Miura, and J. J. Jonas, *Prog. Mater. Sci.*, **60**: 13 (2014).
65. S. Gourdet and F. Montheillet, *Mat. Sci. Eng.*, **283**, Iss. 1–2: 274 (2000).
66. A. Galiyev, R. Kaibyshev, and G. Gottstein, *Acta Mater.*, **49**, Iss. 7: 1199 (2001).
67. Y. Huang and F.J. Humphreys, *Acta Mater.*, **47**, Iss. 7: 2259 (1999).
68. A. Belyakov, K. Tsuzaki, H. Miura, and T. Sakai, *Acta Mater.*, **51**, Iss. 3: 847 (2003).
69. O. Sitdikov, T. Sakai, A. Goloborodko, H. Miura, and R. Kaibyshev, *Philos. Mag.*, **85**, No. 11: 1159 (2005).
70. W. Liu, D. Juul Jensen, and J. J. Morris, *Acta Mater.*, **49**: 3347 (2001).
71. K. Huang and R. E. Loge, *Mater. Des.*, **111**: 548 (2016).
72. A. Belyakov, T. Sakai, H. Miura, and K. Tsuzaki, *Philos. Mag. A*, **81**: 2629 (2001).
73. S. White, *Proc. R. Soc. A*, **283**: 69 (1976).
74. S. E. Ion, F. J. Humphreys, and S. H. White, *Acta Metall.*, **30**: 1909 (1982).
75. L. S. Tyth, Y. Estrin, R. Lapovok, and C. Gu, *Acta Mater.*, **58**, Iss. 5: 1782 (2010).
76. A. Belyakov, Y. Kimura, Y. Adachi, and K. Tsuzak, *Mater. Trans.*, **45**, Iss. 9: 2812 (2004).
77. T. Sakai, A. Belyakov, and H. Miura, *Metall. Mater. Trans. A*, **39**: 2206 (2008).
78. A. Gholinia, F. Humphreys, and P. Prangnell, *Acta Mater.*, **50**, Iss. 18: 4461 (2002).
79. I. E. Volokitina and A. V. Volokitin, *Phys. Met. Metallogr.*, **119**: 917 (2018).
80. G. Kurapov, E. Orlova, I. Volokitina, and A. Turdaliev, *J. Chem. Technol. Metall.*, **51**: 451 (2016).

81. A. V. Volokitin, I. E. Volokitina, and E. A. Panin, *Prog. Phys. Met.*, **23**, Iss. 3: 411 (2022).
82. L. E. Murr, C. S. Niou, J. C. Sanchez, and L. Zernow, *Scripta Met. et Mat.*, **32**: 31 (1995).
83. H. J. McQueen, O. Knustad, N. Ryum, and J. K. Solberg, *Scr. Metall.*, **19**: 73 (1985).
84. G. A. Henshall, M. E. Kassner, and H. J. McQueen, *Metall. Mater. Trans. A*, **23**: 881 (1992).
85. F. J. Humphreys, P. B. Prangnell, J. R. Bowen, A. Gholinia, and C. Harris, *Philos. Trans. R. Soc. A*, **357**, Iss. 1756: 1663 (1999).
86. M. E. Kassner and S. R. Barrabes, *Mater. Sci. Eng. A*, **410**: 152 (2010).